The Astrophysical Journal Letters, 960:L1 (7pp), 2024 January 1 https://doi.org/10.3847/2041-8213/ad0e76

First Detection of an Overmassive Black Hole Galaxy UHZ1: Evidence for Heavy Black Hole Seed Formation from Direct Collapse

Priyamvada Natarajan[1,2,3], Fabio Pacucci[3,4], Angelo Ricarte[3,4], Ákos Bogdán[4], Andy D. Goulding[5], and Nico Cappelluti[6]
[1] Department of Astronomy, Yale University, New Haven, CT 06511, USA; priyamvada.natarajan@yale.edu
[2] Department of Physics, Yale University, New Haven, CT 06520, USA
[3] Black Hole Initiative, Harvard University, 20 Garden Street, Cambridge, MA 02138, USA
[4] Center for Astrophysics, Harvard & Smithsonian, 60 Garden Street, Cambridge, MA 02138, USA
[5] Department of Astrophysical Sciences, Princeton University, Princeton, NJ 08544, USA
[6] Department of Physics, University of Miami, Coral Gables, FL 33124, USA
Received 2023 July 26; revised 2023 November 19; accepted 2023 November 21; published 2023 December 29

Abstract

The recent Chandra-JWST discovery of a quasar in the $z \approx 10.1$ galaxy UHZ1 reveals that accreting supermassive black holes were already in place 470 million years after the Big Bang. The Chandra X-ray source detected in UHZ1 is a Compton-thick quasar with a bolometric luminosity of $L_{\rm bol} \sim 5 \times 10^{45}$ erg s^{-1}, which corresponds to an estimated black hole (BH) mass of $\sim 4 \times 10^7\, M_\odot$, assuming accretion at the Eddington rate. JWST NIRCAM and NIRSpec data yield a stellar mass estimate for UHZ1 comparable to its BH mass. These characteristics are in excellent agreement with prior theoretical predictions for a unique class of transient, high-redshift objects, overmassive black hole galaxies (OBGs) by Natarajan et al., that harbor a heavy initial black hole seed that likely formed from the direct collapse of the gas. Given the excellent agreement between the observed multiwavelength properties of UHZ1 and theoretical model template predictions, we suggest that UHZ1 is the first detected OBG candidate. Our assertion rests on multiple lines of concordant evidence between model predictions and the following observed properties of UHZ1: its X-ray detection and the estimated ratio of the X-ray flux to the IR flux, which is consistent with theoretical expectations for a heavy initial BH seed; its high measured redshift of $z \approx 10.1$, as predicted for the transient OBG stage ($9 < z < 12$); the amplitude and shape of the detected JWST spectral energy distribution (SED) between 1 and 5 μm, which is in very good agreement with simulated template SEDs for OBGs; and the extended JWST morphology of UHZ1, which is suggestive of a recent merge and is also expected for the formation of transient OBGs. As the first OBG candidate, UHZ1 provides compelling evidence for the formation of heavy initial seeds from direct collapse in the early Universe.

Unified Astronomy Thesaurus concepts: Black holes (162); Quasars (1319); Astrophysical black holes (98); Supermassive black holes (1663)

1. Introduction

The origin of the first supermassive black holes (SMBHs) in the Universe remains an open question in astrophysics. Accounting for actively growing SMBHs with masses of $\sim 10^9\, M_\odot$ in detected $z \gtrsim 6$ luminous quasars from light initial seeds has proven to be challenging given the time available for assembling their inferred high masses (see recent review by Fan et al. 2023 and references therein). Given that black holes (BHs) are expected to grow via mergers and accretion over cosmic time (Haehnelt et al. 1998; Pacucci & Loeb 2020), information about their initial seeding is expected to be erased. Therefore, directly accessing the highest-redshift population offers the best prospects (Ricarte & Natarajan 2018; Pacucci & Loeb 2022) to constrain BH seeding models.

A range of theoretical seeding prescriptions operating as early as at $z \sim 20$–25 classified broadly as "light" and "heavy" seeding models have been proposed as starting points to account for the formation of observed SMBHs (Natarajan 2011; Volonteri 2012; Woods et al. 2019). Light seeds are believed to be the remnants of the first generation of stars, the so-called Population III stars, which result in the production of initial BH seeds with 10–100 $M_\odot$ (Madau & Rees 2001).

Heavy seed models, on the other hand, propose the formation of 10^4–$10^5\, M_\odot$ seeds in several possible ways. First, heavy seeds could result from the direct collapse of pregalactic gas disks (Loeb & Rasio 1994; Volonteri & Rees 2005; Begelman et al. 2006; Lodato & Natarajan 2006, 2007).

There are other promising proposed pathways and sites to form DCBH seeds at early epochs (i) from halos with supersonic baryon streaming motions relative to dark matter (Stacy et al. 2011; Schauer et al. 2017); (ii) in highly turbulent halos that are now thought to create the first quasars (Latif et al. 2022); and (iii) from major mergers of massive galaxies (Mayer et al. 2023; Mayer & Bonoli 2019). An additional pathway involves rapid, amplified early growth of originally light seeds that may end up in conducive cosmic environments, such as gas-rich, dense nuclear star clusters (Alexander & Natarajan 2014).

The final stages of the formation of the DCBH have been explored in simulations up to the stage where supermassive stars (SMSs) are produced. Rapid baryon collapse at the center of atomically cooled halos has been demonstrated to produce SMSs (Hosokawa et al. 2013; Woods et al. 2017; Haemmerlé et al. 2018; Herrington et al. 2023) that are then predicted to collapse either by the post-Newtonian general relativity instability or from the depletion of core fuel at the end of

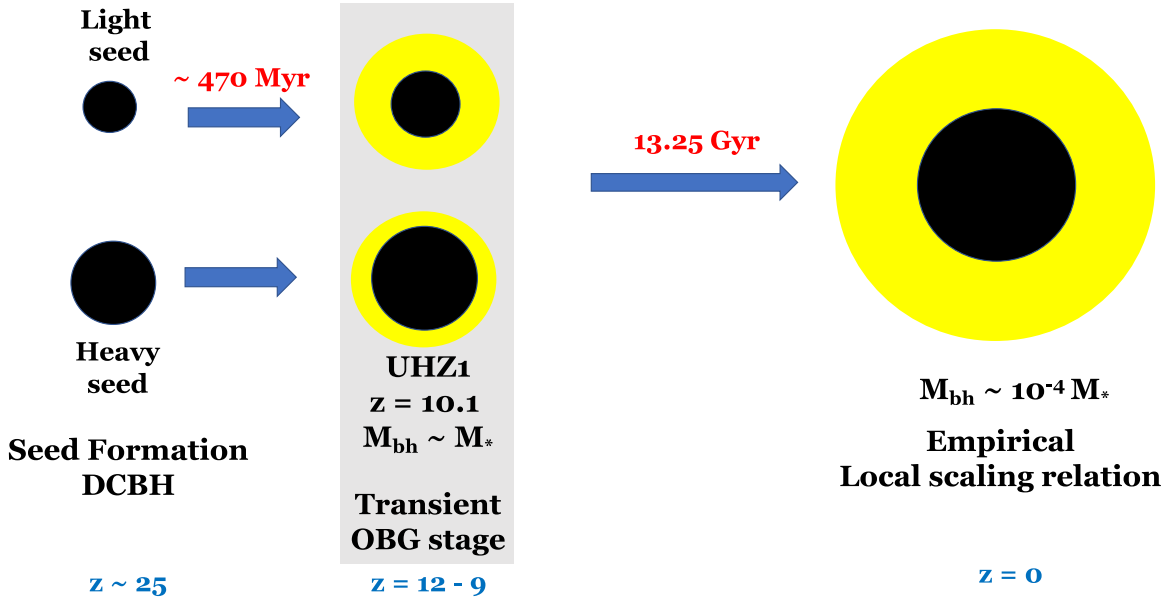

Figure 1. Schematic diagram of the potential assembly history of the OBG candidate UHZ1. The direct collapse of primordial gas disks resulting in the production of heavy initial black hole seeds has been demonstrated to occur feasibly in the setting shown here: satellite DCBH halos that are bound to parent star-forming halos (see Figure 1 in Natarajan et al. 2017). Star formation in the satellite atomic cooling DCBH halo is expected to be suppressed due to the dissociation of molecular hydrogen from the Lyman–Werner radiation produced by the parent galaxy. As a consequence, the OBG is a merger remnant that contains a growing DCBH seed with an initial mass of $\sim 10^4 M_\odot$ with $M_{\rm bh} \geqslant M_*$.

post-main-sequence burning to form DCBHs. These simulations are yet to track the subsequent formation and growth of the BH seed and the stellar component in the host galaxy.

Rapid mergers of light remnants in the early nuclear star clusters could also lead to the formation of heavy seeds at high redshifts as proposed by Devecchi & Volonteri (2009), as well as the runaway collapse of nuclear star clusters as proposed by Davies et al. (2011). In addition to these more conventional theoretical seeding models, primordial black holes (Hawking 1971) that form in the infant Universe have also been explored as potential candidates to account for the origin of initial seeds for SMBHs (see Cappelluti et al. 2022 and references therein), as well as dark stars that are postulated to be powered by dark matter self-annihilation in their cores (Freese et al. 2016).

In this work, we focus on one scenario for DCBH formation in which viable DCBH formation sites in the cold dark matter–dominated cosmogony are pristine atomic cooling halos, satellites bound to the first star-forming galaxies. In these satellite subhalos, gas cooling and fragmentation, and hence star formation are suppressed as the more efficient molecular hydrogen coolant gets rapidly dissociated due to irradiation by the Lyman–Werner photons from the parent star-forming halo (Wise & Abel 2008; Agarwal et al. 2013; Regan et al. 2017; Wise et al. 2019; Patrick et al. 2023).

The satellite DCBH subhalo is then predicted to rapidly merge within ~1–5 Myr with the parent star-forming halo to produce a new, transient class of high-redshift objects, outsize black hole galaxies (OBGs; Agarwal et al. 2013; Natarajan et al. 2017). The merger product, an OBG, would then harbor a growing central heavy BH seed procured from the satellite and the stellar population contributed by the parent galaxy. A schematic outline of the formation process of an OBG is shown in Figure 1. After the merger, the stars and the BH would continue to grow self-consistently as the same gas reservoir that feeds the BH also forms stars. Given that $M_* \sim M_{\rm bh}$ for an OBG (Natarajan 2011; Agarwal et al. 2013; Pacucci et al. 2017a; Visbal & Haiman 2018), this results in a strikingly different BH-to-host galaxy stellar mass ratio than observed in the local Universe, where the mass of the central BH is ~0.1% of the stellar mass (Ferrarese & Merritt 2000; Tremaine et al. 2002).

At present, this is the only scenario in which the entire arc of the formation, early growth of the DCBH seed and properties the stellar population of the host galaxy and its observational consequences in terms of high-redshift multiwavelength signatures via spectral predictions have been predicted. For the other proposed channels for DCBH formation, the detailed exploration of the relationship between the mass of the growing DCBH seed and that of the stars in the host galaxy is awaited and the nature of this relation may well provide the discrimination between the multiple DCBH formation channels. For instance, DCBHs resulting from the major mergers of massive galaxies at extremely high redshifts as proposed by Mayer & Bonoli (2019) are unlikely to lead to the formation of OBGs due to the abundance of stars available in these merger remnant hosts.

Data flowing currently from the JWST are rapidly reshaping our understanding of early galaxy formation with the reported detection of large numbers of faint, distant galaxies at $z > 9$ (Castellano et al. 2022, 2023; Harikane et al. 2023; Naidu et al. 2022; Adams et al. 2023; Atek et al. 2023a, 2023b; Leung et al. 2023), many of which may harbor central BHs (Bogdan et al. 2023; Juodžbalis et al. 2023; Larson et al. 2023; Maiolino et al. 2023).

Utilizing the achromatic nature of gravitational lensing, Bogdan et al. (2023) innovatively deployed Chandra also to study the A2744 field in X-ray wavelengths to detect magnified faint background galaxies and their accreting central BHs. A2744 is a Frontier Fields cluster lens at $z \sim 0.31$ with an extremely well-calibrated lensing mass model.[7] Bogdan et al. (2023) report the (4.2–4.4)σ detection of an X-ray emitting

[7] See, for instance, the six independently derived lensing mass models for this Frontier Fields cluster that are publicly available (https://archive.stsci.edu/prepds/frontier/lensmodels/).

source in the $z \simeq 10.1$ galaxy, UHZ1. The JWST image of UHZ1 appears to be extended, and its redshift has since been spectroscopically confirmed with JWST NIRSpec data as $z \simeq 10.1$ (Goulding et al. 2023). Bogdan et al. (2023) report a best-fit column density of $N_{\rm H} \approx 8^{+\rm inf}_{-7} \times 10^{24}$ cm^{-2} and a corresponding intrinsic 2–10 keV luminosity of $L_{\rm X,int} \approx 9 \times 10^{45}$ erg s^{-1} after correcting for the $\mu = 3.81$ lensing magnification factor at the location of UHZ1. Taken together, these suggest the presence of an obscured, likely Compton-thick, accreting BH in UHZ1.

Given the properties of the unique simultaneous Chandra and JWST detection for UHZ1, we make the case that UHZ1 is the first detected OBG candidate. We demonstrate this by comparing the multiwavelength UHZ1 data in hand with theoretical OBG model template predictions previously reported in Natarajan et al. (2017). We note that its X-ray detection is what uniquely sets UHZ1 apart in contrast to all the other recent JWST detections of high-redshift accreting BHs.

The outline of this paper is as follows: in Section 2, we briefly describe the key ingredients of the models and the procedure used to determine multiwavelength template spectra for OBGs; we present the comparison of UHZ1 data with multiwavelength model predictions of growing early DCBH seeds in Section 3. We conclude with a discussion of the implications of this first detection of an OBG for a deeper understanding of BH seeding channels and the assembly history of early black holes in Section 4.

2. Derivation of OBG Model Templates

We extended and expanded the tracking of early BH seed growth done using the GEMS code presented in Pacucci et al. (2015a, 2016, 2017b), to include the cosmological context of the OBG stage as shown in the schematic in Figure 1 and described in Natarajan et al. (2017). We constructed a library of template multiwavelength spectral models by varying the following key parameters while tracing the formation and evolution of the OBG: (i) the metallicity of the gas and stellar population; (ii) the accretion mode—the standard radiatively efficient thin-disk mode (Eddington limited as it is feedback regulated) and the radiatively inefficient slim disk (super-Eddington accretion is permitted as the accretion is entirely gas supply limited in that instance), and (iii) age of the stellar population. The range of initial conditions for these cases, including gas fraction are adopted from the First Billion Years (FiBY) project cosmological simulation, wherein both DCBH formation and light seed formation sites are selected. Based on the smooth particle hydrodynamics code Gadget, FiBY contains an equal number of gas and dark matter particles (684^3 each; in a box with a comoving 4 Mpc on a side; with gas particle mass of 1253 $M_\odot$ and dark matter particle mass of 6161 $M_\odot$, which permits atomic cooling halos to be well resolved and studied). Further details of the FiBY simulation, including prescriptions adopted for star formation, and Lyman–Werner radiation therefrom and feedback are reported in Agarwal et al. (2014). Initial conditions adopted for feasible BH seed formation sites from fiBY are adopted for the GEMS runs.

The library of model templates for OBGs is generated by simultaneously following the evolution of growing BH seeds (heavy and light) and the accompanying stellar populations with a range of ages and metallicities. The early growth of the BH seed is computed separately using 1D radiation-hydrodynamical models (Pacucci & Ferrara 2015; Pacucci et al. 2015a, 2016, 2017a). These models simulate spherical accretion onto the high-redshift seed BH, and calculate the emitted luminosity self-consistently from the mass accretion rate. The key input parameters for these models are the gas density and metallicity (taken from the fiBY cosmological simulation) and the BH seed mass. The postprocessing spectral analysis is done using CLOUDY (Ferland et al. 2013).

For our models the gas fraction in viable DCBH formation sites and the star formation history of the parent halo are are taken from fiBY (Agarwal et al. 2014). The evolution of the accompanying stellar component is tracked simultaneously and finally combined with that of the growing BH.

Two limiting cases for growth by accretion are implemented to produce a library of models (Pacucci et al. 2015b): standard accretion—which adopts the standard α-disk model that is geometrically thin and optically thick, and hence radiatively efficient with accretion capped at the Eddington rate; and slim-disk accretion, which is characterized by a geometrically thick disk that is radiatively inefficient where radiation pressure is less efficient, quenching gas inflow due to radiation trapping permitting super-Eddington accretion rates. The spectral shape of the output luminosity from accretion onto the BH is determined largely by the geometric properties of the accretion disk. Eddington-limited accretion is the hallmark of thin-disk accretion during which the output luminosity $L_{\rm acc} \propto \dot{M}_{\rm acc}$, where $\dot{M}_{\rm acc}$ is the mass accretion rate. In this highly radiatively efficient regime, the luminosity is feedback limited. Meanwhile, as slim accretion disks result in super-Eddington accretion rates, in this instance, the output $L_{\rm acc} \propto [\ln \dot{M}_{\rm acc}]$. In this radiatively inefficient regime, gas accretion is expected to be supply limited. These two distinct geometries result in dramatically different fluxes mapped out in our models. Postprocessing in CLOUDY utilizes inputs from GEMS at various time slices for light and heavy seeds and includes obscuration. As the accreting BH and stellar component are evolved separately, feedback coupling between them is not taken into account in these models.

The combined contribution of fluxes from the stellar component and both light and heavy accreting seeds is computed in the generated synthetic models derived by combining the pure seed mass evolution followed via GEMS along with the stellar population. The stellar population is modeled using two possibilities: a younger, lower metallicity ($5 \times 10^{-4}\, Z_{M_\odot}$) and an older, higher metallicity population ($5 \times 10^{-2}\, Z_{M_\odot}$), both modeled with a Kroupa initial mass function (IMF). Distinct seeding signatures are seen in the emergent spectrum. The resulting properties for the full parameter space comprising the two seeding scenarios, two accretion models, and two distinct assumptions for the metallicity of the stellar population are presented in detail in Natarajan et al. (2017).

Robust selection criteria for OBGs powered by initially heavy seeds have also been derived, including a preselection to eliminate blue sources, followed by color–color cuts ([F090W − F220W] > 0; − 0.3 < [F200W − F444W] < 0.3) and the ratio of X-ray flux to rest-frame optical flux (FX/F444W $\gg 1$). These cuts sift out OBGs from other bright, high- and low-redshift contaminants in the infrared. OBGs were predicted to have faint but detectable magnitudes of $M_{\rm AB} < 25$ and unambiguously detectable by the NIRCam (Near-Infrared Camera) on JWST. Fainter growing light seed remnants with lower birth masses were

found to have significantly fainter predicted AB magnitudes of $M_{\rm AB} < 31$ by $z \sim 10$.

3. Comparison of UHZ1 with OBG Model Templates

We use the following observed properties of UHZ1 to find a template match from our library of early seed growth models first presented in Natarajan et al. (2017). As reported by Castellano et al. (2022, 2023), UHZ1, magnified by the foreground cluster A2744, has an intrinsic magnitude that renders it detectable with a magnitude of $M_{\rm AB} \sim 27$ and a nearly flat spectral energy distribution (SED) in the observed JWST bands spanning $1-5\,\mu$m. Fitting a Salpeter IMF, Castellano et al. (2023) infer a stellar mass for UHZ1 of $\sim 4 \times 10^7\,M_\odot$, and it is found that combining photometry with JWST NIRSpec data (Goulding et al. 2023) provides a slightly higher stellar mass estimate. An independent fit performed by Atek et al. (2023a) also reports a stellar mass of $\sim 7 \times 10^7\,M_\odot$, making all these estimates broadly consistent with each other. The measured bolometric luminosity from Chandra is $L_{\rm X} \sim 5 \times 10^{45}\,{\rm erg\,s^{-1}}$, yielding a BH mass of $\sim 4 \times 10^{7-8}\,M_\odot$ assuming accretion at the Eddington rate (Bogdan et al. 2023). In addition to these multiwavelength data, the composite JWST image of UHZ1 appears extended. We note that in their SED fit Castellano et al. (2023) were unaware of the presence of an accreting BH. The X-ray detection of UHZ1, combined with JWST flux measurements and recent JWST NIRSpec data, motivates and strongly justifies our exploration of an OBG model match to UHZ1.

We also note the following uncertainties in interpreting the data for UHZ1. As the column density is weakly constrained, the mass estimate for the BH in UHZ1 from X-ray data is also not tightly constrained. Meanwhile, the stellar mass estimate from SED fitting to JWST data also represents a lower limit as current templates do not fully take into account the underlying older stellar population that may be contained in sources like UHZ1.

We note that the current JWST SED fitting for UHZ1 adopted by Castellano et al. (2023) assumes that the observed UV/optical emission derives solely from the stellar component modeled with a Salpeter IMF. This fit was done before the detection of the accreting BH, which is reported to be heavily obscured by Bogdan et al. (2023). With the subsequent knowledge and derived properties of the SMBH hosted in UHZ1 from the X-ray data, we explore whether the rest-frame UV/optical SED and corresponding X-ray flux detected are compatible with our theoretical model templates of OBGs (Natarajan et al. 2017).

We first explore the mass accretion history of the BH in UHZ1, starting from initially light ($100\,M_\odot$) and heavy seeds ($10^4\,M_\odot$) at $z > 20$ to reach the final inferred BH mass of $\sim 10^7\,M_\odot$. An initially light seed with a birth mass of 10–$100\,M_\odot$, would need to steadily accrete at well above the Eddington rate (over $2\times$ the Eddington rate) for roughly 300 million years, while a heavy DCBH seed with an initial birth mass of $10^4\,M_\odot$ could reach the final mass of the BH powering UHZ1 while accreting at just the Eddington rate throughout.

Next, we look at template model matches from our library for the multiwavelength SEDs for UHZ1 for the two possible seeding scenarios; the two assumed accretion models and possibilities for the age and metallicity of the stellar population that bracket the entire permitted parameter space. Our template library includes outputs for the time slice with the largest detectable X-ray flux.

To explain UHZ1 with a light initial seed of $100\,M_\odot$, accreting at super-Eddington rates captured via our slim-disk accretion model, we do not find a template match that simultaneously satisfies JWST and Chandra data for UHZ1. A template that comes somewhat close is the predicted model JWST SED is shown in Figure 2 (gray spectrum) where it is seen that the predicted JWST flux is approximately 2 orders of magnitude lower than observed, resulting in the production of a significantly fainter source, predicted to have $M_{\rm AB} \leqslant 31$, at the sensitivity limit of JWST. Additionally, UHZ1 would have been undetected in X-rays in contradiction to what is seen. Therefore, the simultaneous X-ray and JWST detection of UHZ1 given the final BH mass of $\sim 10^7\,M_\odot$ that is needed to be in place by $z = 10.1$ strongly disfavors UHZ1 as originating from a light seed.

Meanwhile, for a heavy seed origin model for UHZ1 with a seed mass of $10^4\,M_\odot$, we do find a template match from our library that simultaneously satisfies JWST and Chandra data for both assumed high and low metallicity values for the stellar population for a range of permitted stellar ages, as there is a trade-off between these two attributes.

For models where growth is via standard Eddington-limited accretion with a column density of $N_{\rm H} \sim 3 \times 10^{24}\,{\rm cm^{-2}}$: (i) the predicted hard X-ray flux is consistent with the measured value compatible with the inferred column density as shown in Figure 3; (ii) the flux ratio $F_{444}/F_{\rm X} \sim 1$ as expected for OBGs, shown in Figure 4; and (iii) UHZ1 satisfies all the color–color selection criteria for an OBG, also seen in Figure 4. The predicted JWST SED shape and amplitude from this template with an age of 350 Myr for the recently merged stellar population with a low metallicity of $\sim 10^{-3}\,Z_{M_\odot}$ matches the data very well as shown in Figure 2 (red spectrum).

In contrast, we note that for templates with a heavy seed of mass $10^4\,M_\odot$ that subsequently grows via slim-disk accretion at potentially super-Eddington rates limited by the available gas supply, the OBG stage is simply too short-lived. While it could be potentially detectable with JWST for the higher metallicity case (for the stellar population in the host galaxy) due to the lowered X-ray flux from the extremely strong obscuration, such sources would be undetected even with the deepest current X-ray exposures. Besides, with an extremely short predicted lifetime in the OBG stage of ~5–10 Myr, these sources would rapidly transit toward $M_* > M_{\rm bh}$. Once again, our Chandra X-ray detection of UHZ1 rules out this family of templates. We map out the parameter space of template models and tabulate the possibilities for UHZ1 in Table 1.

4. Conclusions and Implications for Early BH Seeding

Despite the theoretical uncertainties in our current understanding of early BH seeding, the detection of even a single high-redshift X-ray quasar, UHZ1, at $z \approx 10.1$ has significant implications as it provides new empirical information on the properties of initial BH seeds and coupling of accreting early BHs and their host galaxies.

With this unique multiwavelength observational data set for UHZ1, we present compelling evidence that it represents the first detection of an OBG, the class of high-redshift galaxies that are seeded with heavy initial BHs, as predicted by Natarajan et al. (2017). As we have shown, all OBG selection criteria are satisfied by UHZ1 with an initial heavy seed mass

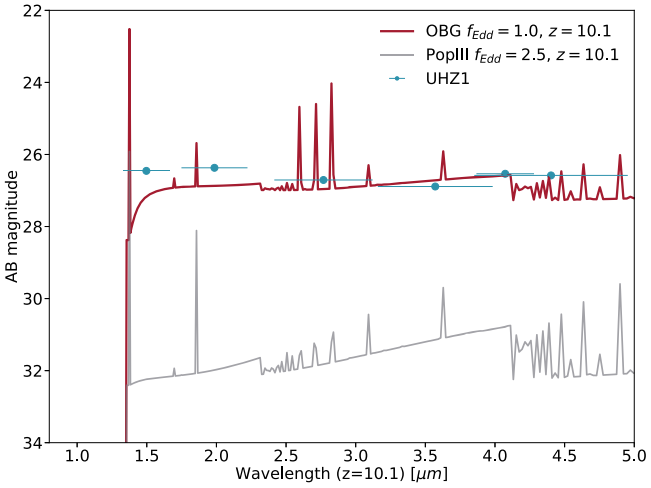

Figure 2. The OBG model match for UHZ1: the model spectrum overplotted here is obtained by growing an initially heavy seed of $\sim 10^4\,M_\odot$ to a final mass of $10^7\,M_\odot$ as estimated for UHZ1 and combining with a young stellar population (age of 350 Myr), low metallicity ($10^{-3}\,Z_{M_\odot}$) with a column density of $\sim 3 \times 10^{24}$ cm^{-2}. The observed near-IR JWST SED for UHZ1 points taken from Castellano et al. (2023) are shown in blue. We note that the overplotted SED template from our library generated with the parameters noted above is very similar to UHZ1.

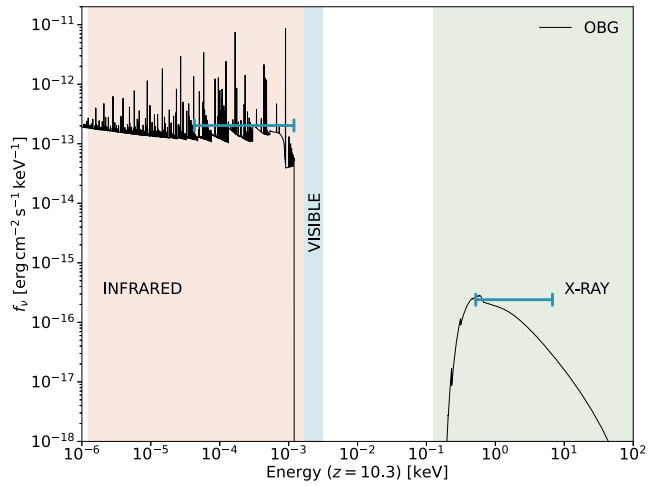

Figure 3. The template match for the multiwavelength SED from our library of OBG models on which we overplot the measured fluxes in the IR from JWST and X-ray from Chandra for UHZ1 shows that they are consistent and well matched. The template that provides this optimal match has the following properties: a heavy initial seed with a mass of $10^4\,M_\odot$; the OBG accreting at the Eddington limit with an age of 350 Myr for the recently merged stellar population with a low metallicity of $\sim 10^{-3}\,Z_\odot$ and a column density of 3×10^{24} cm^{-2}, shown in Figure 2 (in red).

of $10^4\,M_\odot$, and its growth history is compatible with standard Eddington-limited accretion. The best model match from our OBG template library for UHZ1 is therefore provided by a heavy initial seed with a low metallicity for the stellar component and age of $\sim$300 Myr. There is a trade-off between the age and metallicity of the stellar population in OBGs. This degeneracy is well documented more generally for stellar populations at other cosmic epochs as well. As seen from Table 2, none of the light seed models are compatible with observations of UHZ1. We, therefore, claim that UHZ1 offers compelling empirical evidence for the existence of heavy seeds in the early Universe.

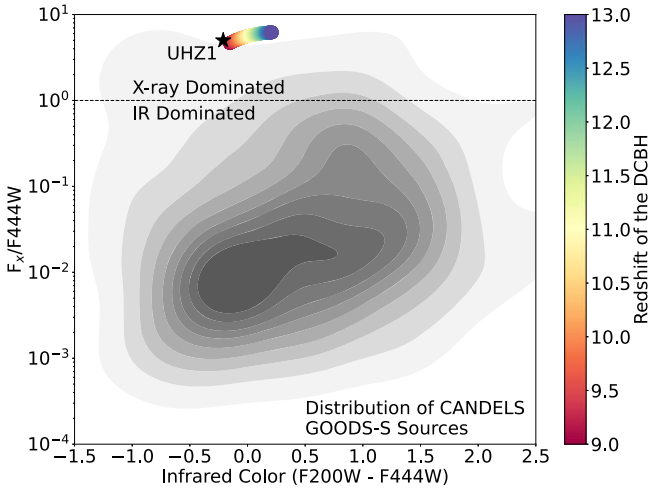

Figure 4. Selection criteria for OBGs: the predicted location of OBGs in color–color space, with the location of UHZ1 marked with a black star.

Table 1
Multiwavelength Detectability of a $10^4 M_\odot$ Seed from Our SED Model Template Library

Metallicity of Stellar Component	Accretion Mode			
	Thin Disk Chandra	Thin Disk JWST	Slim Disk Chandra	Slim Disk JWST
Low Z	✓	✓	X	✓
High Z	✓	✓	X	✓

Table 2
Synopsis of Multiwavelength Detectability for an Initially Light Seed from Our Template Library of Predicted SEDs and Compatibility with Observed Properties of UHZ1

Metallicity of Stellar Component	Accretion Mode			
	Thin Disk Chandra	Thin Disk JWST	Slim Disk Chandra	Slim Disk JWST
Low Z	X	at the limit	X	X
High Z	X	at the limit	X	X

Studies of the BH seeding epoch have thus far been restricted to theoretical explorations. Forming BH seeds ab initio in cosmological simulations and tracking their growth history is extremely challenging. Most simulation suites adopt simple seeding prescriptions to track BH growth and feedback over cosmic time. Detecting the first OBG candidate, UHZ1, offers empirical guidance to inform our heavy seeding theoretical models. As JWST progressively brings the $z > 10$ Universe into view, detecting individual extreme accreting BHs at the earliest epochs is likely to provide new powerful insights in the coming years.

In this work, we are explicitly not making a case for extrapolation of the growth of UHZ1 down to $z = 6$–7. We do not claim it is a likely progenitor for the luminous optically detected Sloan Digital Sky Survey quasars. We are cautious about this as cosmological simulations, the MASSIVEBLACK

suite in particular, have shown that the most massive BH at $z \sim 10$ does not necessarily remain and grow to be the most massive BH by $z = 6$ (Di Matteo et al. 2017, 2023). We emphasize that the details of the larger-scale environment play an important role in shaping the accretion and, therefore, the growth history of BHs. Neither our 1D hydrodynamical BH growth tracking simulations, whose results informed our model templates, nor large cosmological boxes at present adequately capture gas flows in the larger environment of BHs. Conversely, in our current analysis, we are agnostic to the Eddington ratio distributions inferred at lower redshifts for observed X-ray active galactic nuclei (AGNs).

We also refrain from making any number density estimates for OBGs relying on the detection of a single source as models and simulations (Wise et al. 2019; Regan et al. 2020; Whalen et al. 2020) indicate that DCBHs are rare and may be expected to account only for a small fraction of the most luminous quasars detected at $z \sim 6$–7. Estimates of the predicted relative abundance of light and heavy seeds are currently highly uncertain. Lack of information on the occupation fraction of BH seeds and an incomplete census of X-rays from early accretors due to obscured accretion preclude detailed calculations at present. However, a rough back-of-the-envelope estimate given the currently observed JWST fields (UNCOVER, GLASS, and CEERS surveys) and the detection of UHZ1 as the single OBG candidate suggests agreement with the expected number densities at $z \sim 10$ from just the number density of DCBH sites estimated in Natarajan et al. (2017) from simulations of $\sim 10^{-6}$–10^{-7} per Mpc^{-3}.

For accreting high-redshift BHs detected only by JWST so far that are not necessarily OBGs and remain undetected in the deepest X-ray data in hand, one theoretical number density estimate has been attempted using semianalytic models that we caution are also unable to capture the properties of the environment. Trinca et al. (2023) discuss the expected number density of $z > 10$ AGNs in JWST fields with footprints and depths similar to those of UNCOVER/GLASS surveys that probe the A2744 field and arrive at the following estimate for expectations: for the CEERS-like survey $\sim$8 to 21 AGNs at $7 \leqslant z \leqslant 10$; JADES-Deep about 12 to 63 AGNs with $7 \leqslant z \leqslant 10$ and 5 to 32 AGNs at $z \geqslant 10$. As we note in this work, only a small fraction of these high-redshift AGNs will be OBGs and be detected in X-rays as well.

Our simple growth models certainly have limits that translate directly into the range of possibilities that we have mapped out to create our model template library as shown in Table 1. We have made simplifying assumptions—as this is the best we can do now as no current cosmological simulations can form BH seeds ab initio and track their growth and that of their galaxy hosts self-consistently, taking the overall environment into account.

As JWST detects more $z > 9$ accreting BHs in the coming cycles, we plan to analyze those sources, investigate possible X-ray counterparts with Chandra, and develop a deeper understanding of OBGs and heavy seeding physics.

Acknowledgments

P.N. acknowledges support from the Gordon and Betty Moore Foundation and the John Templeton Foundation that fund the Black Hole Initiative (BHI) at Harvard University where she serves as one of the PIs. F.P. acknowledges support from a Clay Fellowship administered by the Smithsonian Astrophysical Observatory. F.P. and A.R also acknowledge support from the BHI. A.B. acknowledges support from the Smithsonian Institution and the Chandra Project through NASA contract NAS8-03060 A.D.G. acknowledges support from NSF/AAG grant 1007094.

ORCID iDs

Priyamvada Natarajan https://orcid.org/0000-0002-5554-8896
Fabio Pacucci https://orcid.org/0000-0001-9879-7780
Angelo Ricarte https://orcid.org/0000-0001-5287-0452
Ákos Bogdán https://orcid.org/0000-0003-0573-7733
Andy D. Goulding https://orcid.org/0000-0003-4700-663X
Nico Cappelluti https://orcid.org/0000-0002-1697-186X

References

Adams, N. J., Conselice, C. J., Ferreira, L., et al. 2023, MNRAS, 518, 4755
Agarwal, B., Dalla Vecchia, C., Johnson, J. L., Khochfar, S., & Paardekooper, J.-P. 2014, MNRAS, 443, 648
Agarwal, B., Davis, A. J., Khochfar, S., Natarajan, P., & Dunlop, J. S. 2013, MNRAS, 432, 3438
Alexander, T., & Natarajan, P. 2014, Sci, 345, 1330
Atek, H., Chemerynska, I., Wang, B., et al. 2023a, MNRAS, 524, 5486
Atek, H., Shuntov, M., Furtak, L. J., et al. 2023b, MNRAS, 519, 1201
Begelman, M. C., Volonteri, M., & Rees, M. J. 2006, MNRAS, 370, 289
Bogdan, A., Goulding, A., Natarajan, P., et al. 2023, NatAs, Advanced Online Publication
Cappelluti, N., Hasinger, G., & Natarajan, P. 2022, ApJ, 926, 205
Castellano, M., Fontana, A., Treu, T., et al. 2022, ApJL, 938, L15
Castellano, M., Fontana, A., Treu, T., et al. 2023, ApJL, 948, L14
Davies, M. B., Miller, M. C., & Bellovary, J. M. 2011, ApJL, 740, L42
Devecchi, B., & Volonteri, M. 2009, ApJ, 694, 302
Di Matteo, T., Angles-Alcazar, D., & Shankar, F. 2023, arXiv:2304.11541
Di Matteo, T., Croft, R. A. C., Feng, Y., Waters, D., & Wilkins, S. 2017, MNRAS, 467, 4243
Fan, X., Bañados, E., & Simcoe, R. A. 2023, ARA&A, 61, 373
Ferland, G. J., Porter, R. L., van Hoof, P. A. M., et al. 2013, RMxAA, 49, 137
Ferrarese, L., & Merritt, D. 2000, ApJL, 539, L9
Freese, K., Rindler-Daller, T., Spolyar, D., & Valluri, M. 2016, RPPh, 79, 066902
Goulding, A. D., Greene, J. E., Setton, D. J., et al. 2023, ApJ, 955, L24
Haehnelt, M. G., Natarajan, P., & Rees, M. J. 1998, MNRAS, 300, 817
Haemmerlé, L., Woods, T. E., Klessen, R. S., Heger, A., & Whalen, D. J. 2018, MNRAS, 474, 2757
Harikane, Y., Ouchi, M., Oguri, M., et al. 2023, ApJS, 265, 5
Hawking, S. 1971, MNRAS, 152, 75
Herrington, N. P., Whalen, D. J., & Woods, T. E. 2023, MNRAS, 521, 463
Hosokawa, T., Yorke, H. W., Inayoshi, K., Omukai, K., & Yoshida, N. 2013, ApJ, 778, 178
Juodžbalis, I., Conselice, C. J., Singh, M., et al. 2023, MNRAS, 525, 1353
Larson, R. L., Finkelstein, S. L., Kocevski, D. D., et al. 2023, ApJL, 953, L29
Latif, M. A., Whalen, D. J., Khochfar, S., Herrington, N. P., & Woods, T. E. 2022, Natur, 607, 48
Leung, G. C. K., Bagley, M. B., Finkelstein, S. L., et al. 2023, ApJL, 945, L46
Lodato, G., & Natarajan, P. 2006, MNRAS, 371, 1813
Lodato, G., & Natarajan, P. 2007, MNRAS, 377, L64
Loeb, A., & Rasio, F. A. 1994, ApJ, 432, 52
Madau, P., & Rees, M. J. 2001, ApJL, 551, L27
Maiolino, R., Scholtz, J., Witstok, J., et al. 2023, arXiv:2305.12492
Mayer, L., & Bonoli, S. 2019, RPPh, 82, 016901
Mayer, L., Capelo, P. R., Zwick, L., & Di Matteo, T. 2023, arXiv:2304.02066
Naidu, R. P., Oesch, P. A., van Dokkum, P., et al. 2022, ApJL, 940, L14
Natarajan, P. 2011, BASI, 39, 145
Natarajan, P., Pacucci, F., Ferrara, A., et al. 2017, ApJ, 838, 117
Pacucci, F., & Ferrara, A. 2015, MNRAS, 448, 104
Pacucci, F., Ferrara, A., Grazian, A., et al. 2016, MNRAS, 459, 1432
Pacucci, F., Ferrara, A., Volonteri, M., & Dubus, G. 2015a, MNRAS, 454, 3771
Pacucci, F., & Loeb, A. 2020, ApJ, 895, 95
Pacucci, F., & Loeb, A. 2022, MNRAS, 509, 1885
Pacucci, F., Natarajan, P., & Ferrara, A. 2017a, ApJL, 835, L36

Pacucci, F., Pallottini, A., Ferrara, A., & Gallerani, S. 2017b, MNRAS, 468, L77
Pacucci, F., Volonteri, M., & Ferrara, A. 2015b, MNRAS, 452, 1922
Patrick, S. J., Whalen, D. J., Latif, M. A., & Elford, J. S. 2023, MNRAS, 522, 3795
Regan, J. A., Visbal, E., Wise, J. H., et al. 2017, NatAs, 1, 0075
Regan, J. A., Wise, J. H., Woods, T. E., et al. 2020, OJAp, 3, 15
Ricarte, A., & Natarajan, P. 2018, MNRAS, 481, 3278
Schauer, A. T. P., Regan, J., Glover, S. C. O., & Klessen, R. S. 2017, MNRAS, 471, 4878
Stacy, A., Bromm, V., & Loeb, A. 2011, ApJL, 730, L1
Tremaine, S., Gebhardt, K., Bender, R., et al. 2002, ApJ, 574, 740
Trinca, A., Schneider, R., Maiolino, R., et al. 2023, MNRAS, 519, 4753
Visbal, E., & Haiman, Z. 2018, ApJL, 865, L9
Volonteri, M. 2012, Sci, 337, 544
Volonteri, M., & Rees, M. J. 2005, ApJ, 633, 624
Whalen, D. J., Surace, M., Bernhardt, C., et al. 2020, ApJL, 897, L16
Wise, J. H., & Abel, T. 2008, ApJ, 685, 40
Wise, J. H., Regan, J. A., O'Shea, B. W., et al. 2019, Natur, 566, 85
Woods, T. E., Agarwal, B., Bromm, V., et al. 2019, PASA, 36, e027
Woods, T. E., Heger, A., Whalen, D. J., Haemmerlé, L., & Klessen, R. S. 2017, ApJL, 842, L6